^{39}K NMR study of the paraelectric-to-incommensurate phase transition in K_2ZnCl_4

B. Topič and U. Haeberlen
Arbeitsgruppe Molekülkristalle, Max-Planck-Institut für Medizinische Forschung, Jahnstrasse 29, D-6900 Heidelberg, Federal Republic of Germany

R. Blinc and S. Žumer
J. Stefan Institute, University of Ljubljana, Jamova 39, YU-61111 Ljubljana, Yugoslavia
(Received 9 July 1990)

The temperature dependence of the quadrupole-perturbed ^{39}K $\frac{1}{2}\rightarrow-\frac{1}{2}$ NMR line shapes has been measured in the paraelectric (PE), incommensurate (*I*), and commensurate (*C*) phases of K_2ZnCl_4 between 600 and 390 K. In the PE phase and the high-temperature part of the *I* phase, fast chemical exchange of the ^{39}K nuclei as well as a diffusive floating of the incommensurate modulation wave take place. In the low-temperature part of the *I* phase the modulation wave becomes solitonlike. The soliton density does not vanish at the *I*-*C* transition but persists well into the *C* phase.

I. INTRODUCTION

K_2ZnCl_4 belongs to the large group of A_2BX_4 crystals which exhibit incommensurate (*I*) phases. It is isostructural with K_2SeO_4 (Ref. 1) with the $ZnCl_4$ tetrahedra replacing the SeO_4 tetrahedra. Above $T_I=553$ K it has the same orthorhombic space group D_{2h}^{16} (*Pcmn*) as K_2SeO_4 with four formula units ($z=4$) per unit cell.[2,3] Between T_I and $T_{c1}=403$ K it is incommensurate with a modulation wave vector $\mathbf{q}=(1-\delta)\mathbf{c}^*/3$, where δ decreases nearly linearly from 0.08 at T_I to 0.03 at T_{c1}. Between T_{c1} and $T_{I'}=148$ K, the phase is commensurate with the orthorhombic space group C_{2v}^9 ($Pc2_1n$) and $z=12$. Here the unit-cell dimension is triplicated along the pseudohexagonal *c* axis just as in K_2SeO_4. Similarly, as in K_2SeO_4, this phase is also an improper ferroelectric one. Between $T_{I'}=148$ K and $T_{c2}=145$ K, there is an intermediate incommensurate phase characterized[4] by a modulation wave vector

$$\mathbf{q}=(0.5\pm\delta)\mathbf{a}^*+0.5\mathbf{b}^* .$$

At $T_{c2}=145$ K, there is a transition to another commensurate phase[5] which is monoclinic with both the *a* and the *b* lattice parameters doubled and with $z=24$. The space group of this phase was suggested to be $C_s^4(Cc)$.[6]

In contrast to K_2SeO_4, neutron-scattering studies[3] did not reveal a soft optic mode in the normal phase above T_I. Instead, diffuse scattering was observed. Raman-scattering studies by Quilichini *et al.*[7] similarly showed that, above 500 K, the amplitudon is superimposed on a broad quasielastic background which decreases rapidly with decreasing temperature. Another unusual feature of K_2ZnCl_4 is the presence of rather large thermal hysteresis and memory effects[8] within the *I* phase and the extremely slow relaxation of the dielectric constant where time constants of many hours[9] have been observed.

In order to throw some light on the microscopic origin of these effects as well as on the nature of the modulation wave in the high-temperature incommensurate phase, we decided to study the quadrupole perturbed ^{39}K NMR spectra of K_2ZnCl_4. We particularly hoped that a comparison with the ^{39}K data in isostructural K_2SeO_4 (Ref. 1) might prove useful in understanding the differences in the molecular dynamics of these two systems and elucidate the origin of the memory effects in K_2ZnCl_4.

II. EXPERIMENT

Fourier-transformed ^{39}K NMR spin-echo spectra were recorded in a superconducting magnet at a Larmor frequency of $\nu_L=16.628$ MHz. Depending on the temperature and orientation of the crystal, between 400 and 2000 echoes were accumulated. The temperature instability over the measuring period was less than 0.5 K.

III. THEORY

The magnetic resonance line shape in the *I* phase strongly depends on the nature of the incommensurate modulation wave. The changes in the electric-field-gradient (EFG) tensor induced by a static incommensurate modulation wave at the position of the αth nucleus in the *l*th paraelectric unit cell can be expressed[10] as a power series in the displacement vectors

$$V=V_0+V_1+V_2+V_3+\cdots , \tag{1a}$$

where

$$V_1=\sum_j(\nabla_jV)_0\mathbf{u}_j , \tag{1b}$$

$$V_2=\sum_j\sum_{j'}\mathbf{u}_{j'}\nabla_{j'}(\nabla_jV)_0\mathbf{u}_j , \tag{1c}$$

$$V_3=\sum_j\sum_{j'}\sum_{j''}\mathbf{u}_{j''}\nabla_{j''}[\mathbf{u}_{j'}\nabla_{j'}(\nabla_iV)_0\mathbf{u}_j] , \tag{1d}$$

with ∇_j standing for the gradient operator and the index

0 for the value of V in the paraelectric phase. The index j, counting the site of the observed nucleus, has been omitted. The real displacement $\mathbf{u}_j$ of the αth nucleus is given by an admixture of the symmetric and the antisymmetric components of the modulation wave[10]

$$\mathbf{u}_j=\mathbf{u}^c_{0\alpha}\cos\phi(x_j)+\mathbf{u}^s_{0\alpha}\sin\phi(x_j)\ . \tag{2}$$

The components of the real displacement vector u_{jK} ($k=x,y,z$) can be now expressed as

$$u_{jK}=u_{0\alpha k}\cos[\phi(x_j)+\phi^{(0)}_{\alpha k}],\quad k=x,y,z\ , \tag{3}$$

where the phase shift $\phi^{(0)}_{\alpha k}$, introduced to eliminate the sine terms, is different for different nuclei in the unit cell. Here $\phi(x)=\mathbf{q}_c\mathbf{x}_\alpha+\varphi(x)$ with $\mathbf{q}_c$ being the modulation wave vector in the commensurate (C) phase, i.e., $\mathbf{c}^*/3$, and $\varphi(x)$ standing for a solution of the sine-Gordon equation. $\mathbf{x}_\alpha(l)=\mathbf{x}_{0\alpha}+l\mathbf{a}$, $l=0,1,2,3,\ldots$, where $\mathbf{x}_{0\alpha}$ describes the position of the αth nucleus in the lth unit cell. In the plane-wave limit, $\varphi(x)$ becomes a linear function of the x coordinate.

The quadrupole shift of the NMR frequency from its paraelectric phase value ν_0 can now be, in this nonlocal model, expressed as

$$\nu(x)=\nu_0+\nu_1\cos[\phi(x)-\phi_1]+\nu_2'+\nu_2''\cos\{2[\phi(x)-\phi_1]-\phi_2\}+\cdots\ , \tag{4}$$

where $\nu_1=\nu_{10}A$, $\nu_2'=\nu_{20}'A^2$, $\nu_2''=\nu_{20}''A^2$, whereas ϕ_1 and ϕ_2 are initial phases. The amplitude of the modulation wave is $A=[(T_I-T)/T_I)]^\beta$ whereas β is a critical exponent. As it has been pointed out recently,[11] strictly speaking, the critical exponent for ν_2' and ν_2'' is not 2β but rather $2\beta-\alpha-\phi$, where $\alpha=-0.007$ is the specific heat and $\phi=1.175$ the crossover exponent. For most practical purposes, however, this correction is much smaller than the experimental uncertainty and hence can be neglected.

It should be noted that, in the case of quadrupole perturbed nuclear magnetic resonance, the expansion coefficients ν_{10}, ν_{20}', and ν_{20}'' depend on the orientation of the external magnetic field with respect to the crystal axes.

The spatial dependence of the resonance frequency results in an inhomogeneous frequency distribution

$$f(\nu)=\text{const}\times\frac{1}{d\nu/dx}=\text{const}\times\frac{1}{(d\nu/d\varphi)(d\varphi/dx)}\ . \tag{5}$$

In the plane-wave limit $d\varphi/dx=\text{const}$ and $f(\nu)$ will exhibit singularities when $d\nu/d\varphi=0$. It should be noted that the function $\nu=\nu(\varphi)$ has several branches which must be all taken into account in the evaluation of the frequency distribution (5).

In the simplest linear case ($\nu_{10}\neq0$, $\nu_{20}'=\nu_{20}''=0$), the incommensurate frequency distribution is given by[12]

$$f(\nu)=\text{const}\times\frac{1}{[\nu_1^2-(\nu-\nu_0)^2]^{1/2}}\ . \tag{6}$$

The splitting $\Delta\nu=2\nu_1$ between the two edge singularities at $\nu_T=\nu-\nu_0=\pm\nu_1$ increases with the critical exponent β as it is proportional to the amplitude of the modulation wave.

The NMR line shape is rather different in the case of chemical exchange of nuclei between the various lattice sites. Let us discuss the simplest case of chemical exchange between two chemically nonequivalent lattice sites A and B. In such a case the Hamiltonian—which is the sum of a Zeeman term $\mathcal{H}_Z$ and a quadrupolar term $\mathcal{H}_Q$—becomes time dependent

$$\mathcal{H}(t)=\mathcal{H}_Z+\mathcal{H}_Q(t) \tag{7a}$$

as

$$\mathcal{H}_Q(t)=\mathcal{H}_{QA}[1+p(t)]/2+\mathcal{H}_{QB}[1-p(t)]/2\ . \tag{7b}$$

The function $p(t)$ randomly takes on the values $+1$ and -1 describing the fraction of time a given nucleus spends in the A and B sites, respectively. Since we deal with a random Markovian process, we have

$$\langle p(t)\rangle=0,\quad p^2(t)=1 \tag{8a}$$

and

$$\langle p(0)p(t)\rangle=e^{-t/\tau}\ . \tag{8b}$$

For sufficiently slow adiabatic processes, the NMR frequency ν becomes time dependent

$$\nu(t)=\nu_L+\Delta\nu(t)\ . \tag{9}$$

In the following we shall, for sake of simplicity, omit the Larmor frequency ν_L. The angular dependence of the second-order quadrupolar shift $\Delta\nu_i(\vartheta)$ of the central $\frac{1}{2}\rightarrow-\frac{1}{2}$ NMR line of a ^{39}K nucleus ($I=\frac{3}{2}$) is given here by

$$\Delta\nu_i(t,\vartheta)=\frac{1}{\nu_L}[A_i+B_i\cos(2\vartheta_i)+C_i\sin(2\vartheta_i)+D_i\cos(4\vartheta_i)+E_i\sin(4\vartheta_i)]\ , \tag{10}$$

where the coefficients[13] A, B, C, D, E are now time dependent. ϑ_i describes the orientation of the external magnetic field with respect to the crystal axes and $i=a,b,c$ label the rotation axes. The expression for D_i, for instance, can be written[13] as

$$D_i=\tfrac{3}{32}(eQ/h)^2[\tfrac{1}{4}(V_{jj}-V_{kk})^2-V_{jk}^2]\ , \tag{11}$$

where $i=a$, $j=b$, and $k=c$ and D_i as well as D_k are obtained by cyclic permutation of the indices. The EFG tensor components V_{jk} are, in view of chemical exchange time dependence, given by

$$V_{jk}^2(t)=\left[V_{jk,A}\frac{1+p(t)}{2}+V_{jk,B}\frac{1-p(t)}{2}\right]^2\ . \tag{12a}$$

Since $p^2=1$, this reduces to

$$V_{jk}^2(t)=V_{jk,A}^2\frac{1+p(t)}{2}+V_{jk,B}^2\frac{1-p(t)}{2}\ , \tag{12b}$$

resulting in

$$D(t)=D_A\frac{1+p(t)}{2}+D_B\frac{1-p(t)}{2} \tag{13a}$$

and

$$\nu[p(t)]=\nu_A\frac{1+p(t)}{2}+\nu_B\frac{1-p(t)}{2} . \quad (13b)$$

The adiabatic NMR line shape is now given by

$$f(\omega)=\int G(t)e^{i\omega t}dt , \quad (14)$$

where

$$G(t)=\left\langle\frac{1}{2\pi}\int_0^{2\pi}d\phi\exp\left[i2\pi\int_0^t\nu[\phi,p(t')]dt\right]\right\rangle_p . \quad (15)$$

And $\nu[\phi,p(t')]$ is given by expression (13b) with $\nu_A(\phi)$ and $\nu_B(\phi)$ having the form of expression (4) with different coefficients. For $(\nu_A-\nu_B)\tau\ll 1$, the spectrum will consist of a single line. With increasing τ the spectrum will broaden and eventually split into two lines if $(\nu_A-\nu_B)\tau\gg 1$. In contrast to the static case, the line shape will not show edge singularities but will be Lorentzian as long as τ is short enough to influence the spectra.

In the low-temperature part of the I phase, motional effects should not be important. Here, however, the plane-wave approximation is expected to break down and $\varphi(x)$ becomes a nonlinear function of x. Additional "commensurate" lines will appear whenever

$$\frac{d\varphi}{dx}\to 0$$

and the intensity of the "edge singularities," where $d\nu/d\varphi=0$, will be reduced.

In the constant-amplitude approximation, one finds[13] $d\varphi/dx$ as

$$\frac{d\varphi}{dx}=\text{const}\times\{\Delta^2+\cos^2[n(\varphi-\phi_0)]\}^{1/2} , \quad (16a)$$

where $n=6$ for K_2ZnCl_4 and Δ^2 is related to the soliton density n_s by

$$n_s=\frac{\pi/2}{K(k)} \quad (16b)$$

with

$$k^2=\frac{1}{1+\Delta^2},\quad K(k)=\int_0^{\pi/2}d\phi\frac{1}{(1-k^2\sin^2\phi)^{1/2}} . \quad (16c)$$

For $\Delta\to 0$ up to n, new C lines will appear when

$$\cos^2[n(\varphi-\phi_0)]=0 ,$$

i.e., when

$$\varphi=(2m+1)\pi/n+\phi_0,\quad m=0,1,2,\ldots,n-1 . \quad (16d)$$

IV. RESULTS AND DISCUSSION

The paraelectric unit cell of K_2ZnCl_4 contains eight K sites which are pairwise magnetically equivalent because of the presence of inversion centers. All K atoms lie on mirror planes perpendicular to the crystal b axis. From symmetry considerations, one can thus deduce that the ^{39}K EFG tensors have—in the crystal-axes fixed frame—the following form:

$$V_0=\begin{bmatrix} V_{aa} & 0 & V_{ac}\\ 0 & V_{bb} & 0\\ V_{ac} & 0 & V_{cc}\end{bmatrix} . \quad (17)$$

There are two sets of chemically nonequivalent K sites, K(1) and K(2) with different eigenvalues. The K(1) ions are surrounded by 11 Cl atoms whereas the K(2) ions are surrounded by only 9 chlorines. Because K(2) is surrounded less symmetrically by fewer and nearer ligands than K(1), we expect, on the basis of point-charge calculations, that the quadrupole coupling constant e^2qQ/h and the asymmetry parameter η of K(1) is smaller than that of K(2) in complete analogy to the situation in K_2SeO_4.[1] Based on the structural data, one thus expects four ^{39}K $\frac{1}{2}\to-\frac{1}{2}$ NMR lines for the rotation $\mathbf{b}\perp\mathbf{B}_0$ and only two, corresponding to K(1) and K(2), for rotations $\mathbf{a}\perp\mathbf{B}_0$ and $\mathbf{c}\perp\mathbf{B}_0$. Physically nonequivalent but chemically equivalent nuclei will, in the $\mathbf{a}\perp\mathbf{B}_0$ and $\mathbf{c}\perp\mathbf{B}_0$ rotations, give rise to one common line.

In fact, only one ^{39}K $\frac{1}{2}\to-\frac{1}{2}$ NMR line is seen for $T>T_I$ and the high-temperature part of the I phase for the $\mathbf{c}\perp\mathbf{B}_0$ as well as the $\mathbf{b}\perp\mathbf{B}_0$ and $\mathbf{a}\perp\mathbf{B}_0$ orientations (Fig. 1). This is completely different from the situation in K_2SeO_4. It means that, as far as the electric-field-gradient tensor is concerned, all ^{39}K sites in the paraelectric and high-temperature parts of the I phase of K_2ZnCl_4 are equivalent. The corresponding ^{39}K EFG tensor in the crystal fixed a,b,c frame is

$$V(^{39}K)=\begin{bmatrix} 0.190 & 0 & 0\\ 0 & 0.247 & 0\\ 0 & 0 & -0.437\end{bmatrix}\text{ MHz},\quad T>T_I .$$

Both the ^{39}K quadrupole coupling constant $e^2qQ/h=0.437$ MHz and the asymmetry parameter

$$\eta=\frac{V_{xx}-V_{yy}}{V_{zz}}=0.13$$

are considerably smaller than the corresponding values for the K(1) and K(2) sites in K_2SeO_4.[1]

There are two possible explanations for this apparent discrepancy between the structural and the NMR data.

(i) The crystal structure of the paralectric phase of

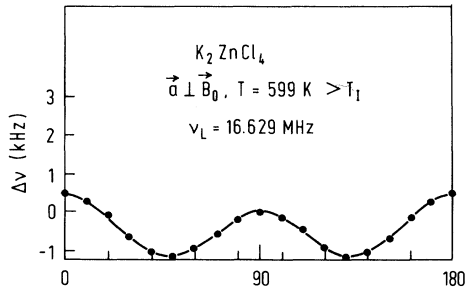

FIG. 1. Angular dependence of the ^{39}K $\frac{1}{2}\to-\frac{1}{2}$ NMR transitions in the paraelectric phase of K_2ZnCl_4.

K_2ZnCl_4 is not isomorphous with K_2SeO_4 and the x-ray determination is not correct.

(ii) A fast chemical exchange between the various K sites takes place so that all K sites in the unit cell are equivalent on the NMR time scale for a high enough temperature and the off-diagonal elements V_{ac} are averaged out.

This last explanation can only be understood if K_2ZnCl_4 is a kind of a superionic conductor at high temperatures. In such a case, rapid translational diffusion of the K^+ ions takes place and the ^+K ions see, as far as NMR is concerned, only the time-averaged and not the instantaneous value of the various EFG tensors. The anomalous temperature dependence of the ^{39}K NMR $\frac{1}{2}\rightarrow-\frac{1}{2}$ spectra strongly supports the second (ii) of these two possibilities (Fig. 2).

The narrow paraelectric ^{39}K $\frac{1}{2}\rightarrow-\frac{1}{2}$ NMR line already starts to broaden far above T_I (Figs. 2 and 3).

On further cooling, the paraelectric ^{39}K $\frac{1}{2}\rightarrow-\frac{1}{2}$ NMR line splits at T_I into two lines (Fig. 3). The line shape is not the one expected for an I phase as no characteristic edge singularities are seen. The splitting increases with decreasing temperature (Fig. 3). A plot of $\log\Delta\nu$ against $T-T_I$ yields a critical exponent $\beta_{\text{eff}}=0.75$ which is much higher than the one expected for I systems ($\beta=0.35$) (inset to Fig. 3). At $T=493$ K, each of the two lines splits again and the line shape becomes characteristic of an incommensurate phase with a plane-wave-type modulation.

This additional splitting increases as well with decreasing temperature. On approaching the lock-in temperature $T_c=130$ K, extra peaks appear which may be ascribed to commensurate (C) regions between phase solitons within the I phase. This demonstrates that a transition from a plane-wave modulation regime to a broad soliton modulation regime[10] takes place in the low-T part of the I phase in K_2ZnCl_4 similarly to K_2SeO_4 (Fig. 5). The C lines continue into the C phase below T_c whereas the incommensurate edge singularities not coinciding with the C lines disappear.

When we tried to describe the temperature dependence of the ^{39}K NMR line shape with the model outlined in Sec. III, we noticed that this model is still oversimplified. Whereas thermally activated ^{39}K chemical exchange can account for the fact that all ^{39}K sites are equivalent at high temperatures and the onset of the incommensurate modulation can explain the line shape and line splittings in the low-temperature part of the I phase and in the C phase, these two mechanisms together cannot account for the behavior around T_I. The point is that the ^{39}K NMR lines start to broaden before the lines split due to the incommensurate modulation. If this broadening would be due to chemical exchange, the various ^{39}K sites in the unit cell should become inequivalent immediately below T_I, which is not the case (Figs. 1–3). Thus, it is obvious that, in addition to chemical exchange, a second much slower motional process is present in the region around T_I. We believe that this second process is a collective diffusive motion of the modulation wave which averages out the incommensurate splitting of the NMR line immediately below T_I. The onset of the I phase is thus

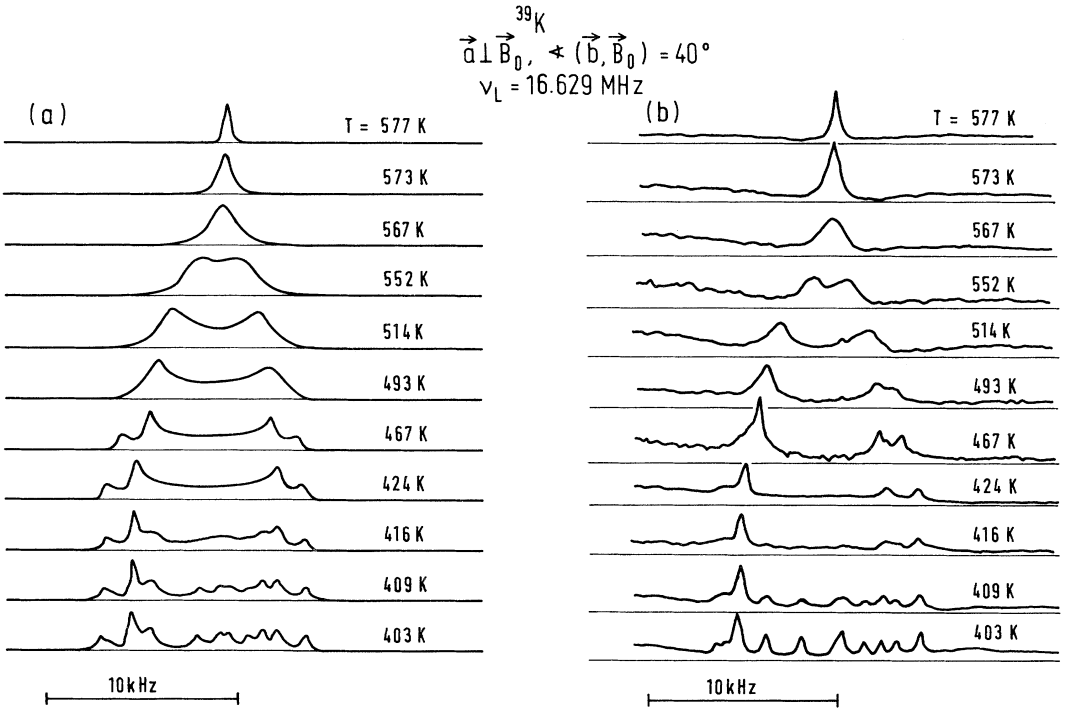

FIG. 2. Temperature dependence of the ^{39}K $\frac{1}{2}\rightarrow-\frac{1}{2}$ NMR line shape in K_2ZnCl_4 in the paraelectric, incommensurate, and commensurate phases: (a) theory, (b) experiment.

demonstrated here first by the broadening of the NMR line. Only well below T_I, when the diffusive sliding of the modulation wave freezes out, the characteristic incommensurate splitting of the NMR line appears (Figs. 2 and 3). This also explains the fact that the splitting of the NMR lines does not coincide with T_I determined by x-ray scattering which is insensitive to the sliding of the modulation wave and chemical exchange.

At still lower temperatures, chemical exchange also freezes out so that the various ^{39}K sites become inequivalent on the NMR time scale resulting in an additional splitting of the NMR spectra (Fig. 3). The number of inequivalent K sites now agrees with the predictions based on x-ray structure determination.

In order to describe the above processes quantitatively, we relaxed the requirement that the modulation wave is static and allowed in expression (4) for thermal phase fluctuations $\phi \rightarrow \phi(t)$, where

$$\phi(t)=\tilde{\phi}_0+\partial\phi(t) \ . \tag{18}$$

Phase fluctuations are related to fluctuations in the position of the modulation wave by $\Delta x=\delta\phi/k_I$, where k_I is the modulation wave vector.

Expression (15) is now changed into

$$G(t)=\left\langle \frac{1}{2\pi}\int_0^{2\pi} d\tilde{\phi}_0 \exp\left[2i\pi\int_0^t \nu(\tilde{\phi}_0,\delta\phi(t'),p(t'))dt'\right]\right\rangle_{p,\delta\phi} , \tag{19}$$

where the two random processes described by $p(t')$ and $\delta\phi(t')$ are assumed to be independent.

The temperature dependence of the ^{39}K NMR line shapes and frequency splittings of K_2ZnCl_4 (Figs. 2 and 3) can now be described by expressions (19), (13b), and (4), where $\nu_{0A}=-0.6$ kHz, $\nu'_{20A}=-0.8$ kHz, $\nu_{10A}=5.5$ kHz, $\nu''_{20A}=-1.3$ kHz, $\phi_{1A}=38°$, $\phi_{2A}=40°$, $\nu_{0B}=0.6$ kHz, $\nu'_{20B}=-2.4$ kHz, $\nu_{10B}=5.5$ kHz, $\nu''_{20B}=1.3$ kHz,

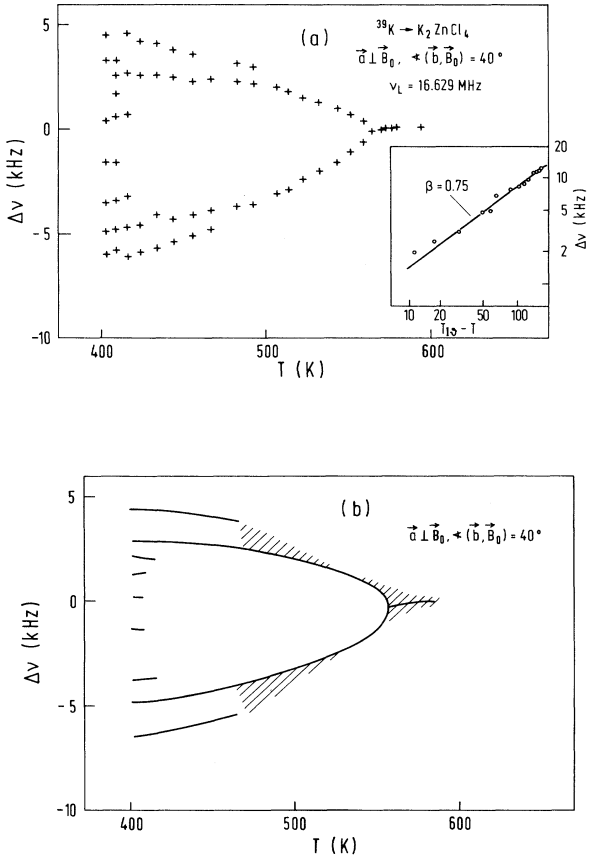

FIG. 3. (a) Temperature dependence of the splitting of the ^{39}K $\frac{1}{2} \rightarrow -\frac{1}{2}$ NMR line in K_2ZnCl_4. The inset shows $\log\Delta\nu$ vs $\log T_I - T$. (b) The theoretical fit is obtained according to expressions (4) and (13)–(16) and parameters described in the text. In the shaded regions a significant broadening of the NMR lines due to chemical exchange and modulation wave floating takes place.

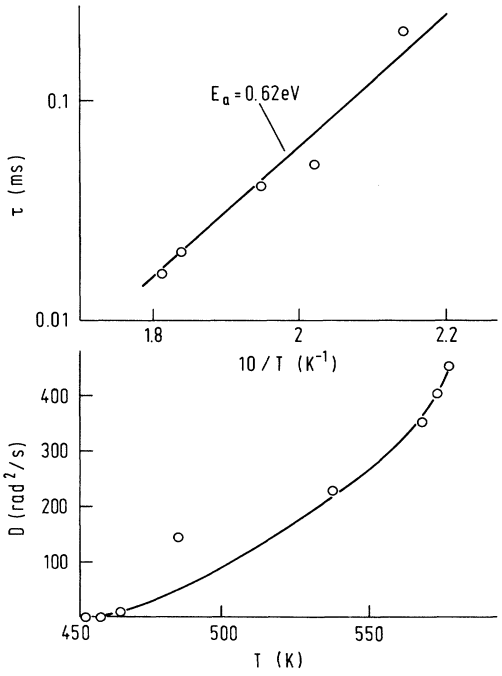

FIG. 4. (a) Temperature dependence of the correlation time for nuclear exchange τ between the K(1) and K(2) sites as deduced from the line-shape fit. (b) Temperature dependence of the diffusion constant for phase fluctuations of the modulation wave.

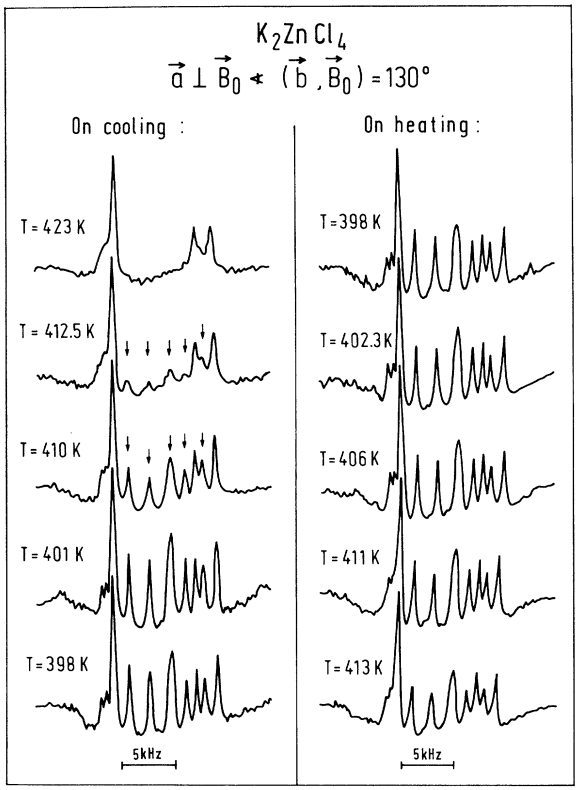

FIG. 5. ^{39}K NMR line shapes in K_2ZnCl_4 close to the *I-C* transition showing the transition from the plane wave to the soliton-like modulation regime. The onset of the "commensurate" lines is designated by arrows.

$\phi_{1B}=2°$, $\phi_{2B}=20°$, and $\beta=0.35$. Expression (19) was evaluated numerically via a computer simulation of the random functions $p(t')$ and $\delta\phi(t')$. For $\delta\phi(t')$ the best fit was obtained for a random-walk-type process with $\langle \delta\phi^2(t) \rangle = 2Dt$. The temperature dependences of the correlation time for chemical exchange τ and of the constant D characterizing the diffusive motion of the modulation wave are presented in Figs. 4(a) and 4(b).

In the low-temperature part of the *I* phase (Fig. 5), the phase of the modulation wave becomes a nonlinear function of x and additional "commensurate" lines appear in the NMR spectrum. The spectra are now described by expressions (4), (5), and (16a)–(16d). The temperature dependence of the soliton density n_s—measuring the fraction of nuclei in the incommensurate domain walls, i.e., discommensurations—is presented in Fig. 6. It is obtained from a comparison of experimental and theoretical line shapes. From T_I down to 333 K we are in the plane-wave limit and $n_s=1$. At 323 K, $n_s=0.8$ and rapidly decreases on approaching T_c. Close to T_c, $n_s=0.15$. This value of n_s persists on cooling into the *C* phase below T_c demonstrating the presence of a, probably metastable, chaotic phase intermediate between the *I* phase and the true *C* phase.[14]

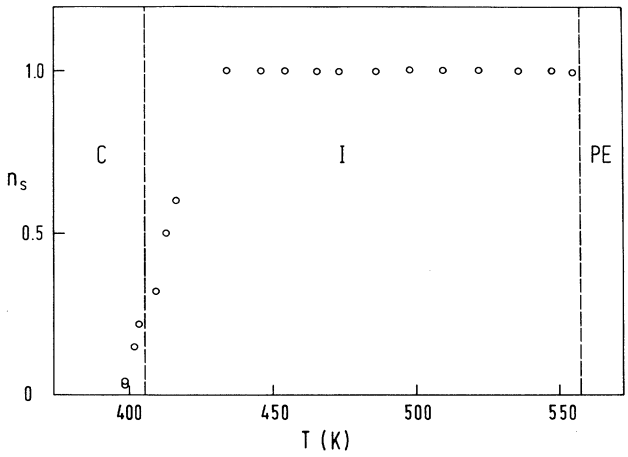

FIG. 6. Temperature dependence of the soliton density n_s in K_2ZnCl_4.

The observed T dependence of the soliton density n_s in K_2ZnCl_4 is thus similar to the one observed in Rb_2ZnCl_4,[15] Rb_2ZnBr_4,[16] and K_2SeO_4.[17] What is specific for K_2ZnCl_4 is the presence of fast chemical exchange of ^{39}K nuclei in the paraelectric phase and the high-T part of the *I* phase reflecting the superionic conductivity of this system as well as a much slower diffusive floating of the modulation wave in the region around T_I.

The above results suggest that the anomalous memory and thermal hysteresis effects observed[8] in the *I* phase of K_2ZnCl_4 may be the result of the interaction of defects—created by the thermal translational diffusion and superionic conductivity of the K^+ ions—with the incommensurate modulation wave. It is interesting to note that diffusion of Na^+ ions and Na^+ vacancies has been, similarly, recently suggested to be responsible for the observed memory effects in the *I* phase of barium sodium niobate.[18]

[1]See, for instance, B. Topič, A. von Kienlin, A. Gölzhäuser, U. Haeberlen, and R. Blinc, Phys. Rev. B **38**, 8625 (1988), and references therein.
[2]A. Kalman, J. S. Stephens, and D. W. S. Cruishank, Acta Crystallogr. B **26**, 1451 (1971).
[3]K. Gesi and M. Iizumi, J. Phys. Soc. Jpn. **53**, 4271 (1984); see also, J. Phys. Soc. Lett. **46**, 697 (1979).
[4]K. Gesi, J. Phys. Soc. Jpn. **59**, 416 (1990).
[5]F. Milia, R. Kind, and J. Slak, Phys. Rev. B **27**, 6662 (1983).
[6]V. Dvorak and R. Kind, Phys. Status Solidi B **107**, K109 (1981).
[7]M. Quilichini, J. P. Mathieu, M. L. Postollec, and N. Toupry, J. Phys. (Paris) **43**, 787 (1982).
[8]H. Mashiyama and H. Kasatani, Jpn. J. Appl. Phys. **24**, S24-2,

802 (1985); J. Phys. Soc. Jpn. **56**, 3347 (1987).
[9]H. G. Unruh, Ferroelectrics **53**, 319 (1984).
[10]R. Blinc, J. Seliger, and S. Žumer, J. Phys. C **18**, 2313 (1985).
[11]R. Walisch, J. M. Perez-Mato, and J. Petersson, Phys. Rev. B **40**, 10 747 (1989).
[12]R. Blinc, Phys. Rep. **79**, 331 (1981).
[13]V. Rutar, J. Seliger, B. Topič, R. Blinc, and I. P. Aleksandrova, Phys. Rev. B **24**, 2397 (1981).
[14]J. C. Toledano, J. Schneck, and G. Errandonea, in *Incommensurate Phases in Dielectrics, 2, Materials,* edited by R. Blinc and A. P. Levanyuk (North-Holland, Amsterdam, 1986), p. 236.
[15]R. Blinc, V. Rutar, B. Topič, S. Žumer, J. Seliger, I. P. Aleksandrova, and F. Milia, J. Phys. C **19**, 3421 (1981).
[16]R. Blinc, V. Rutar, B. Topič, F. Milia, and Th. Rasing, Phys. Rev. B **33**, 1721 (1986).
[17]B. Topič, U. Haeberlen, and R. Blinc, Phys. Rev. B **42**, 7790 (1990).
[18]J. Dolinšek, R. Blinc, and J. Schneck, Solid State Commun. **70**, 1077 (1989).